83-GT-224

THE AMERICAN SOCIETY OF MECHANICAL ENGINEERS
345 E. 47 St., New York, N.Y. 10017





# STIFFNESS DERIVATIVE FINITE ELEMENT TECHNIQUE TO DETERMINE NODAL WEIGHT FUNCTIONS WITH SINGULARITY ELEMENTS

George T. Sha, Ph.D.

Staff Development Engineer
Detroit Diesel Allison
Division of General Motors Corporation
P.O. Box 894
Indianapolis, Indiana 46206



## ABSTRACT

The use of the stiffness derivative technique coupled with "quarter-point" singular crack-tip elements permits very efficient finite element determination of both stress intensity factors and nodal weight functions. Two-dimensional results are presented in this paper to demonstrate that accurate stress intensity factors and nodal weight functions can be obtained from relatively coarse mesh models by coupling the stiffness derivative technique with singular elements.

The principle of linear superposition implies that the calculation of stress intensity factors and nodal weight functions with crack-face loading, $\sigma(r_s)$, is equivalent to loading the cracked body with remote loads, which produces $\sigma(r_s)$ on the prospective crack face in the absence of crack. The verification of this equivalency is made numerically, using the virtual crack extension technique. Load independent nodal weight functions for two-dimensional crack geometry is demonstrated on various remote and crack-face loading conditions. The efficient calculation of stress intensity factors with the use of the "uncracked" stress field and the crack-face nodal weight functions is also illustrated.

In order to facilitate the utilization of the discretized crack-face nodal weight functions, an approach was developed for two-dimensional crack problems. Approximations of the crack-face nodal weight functions as a function of distance, $(r_s)$, from crack-tip has been successfully demonstrated by the following equation:

$$h(a,r_s) = \frac{A(a)}{\sqrt{r_s}} + B(a) + C(a)\sqrt{r_s} + D(a)\, r_s$$

Coefficients A(a), B(a), C(a) and D(a), which are functions of crack length (a), can be obtained by least-squares fitting procedures. The crack-face nodal weight functions for a new crack geometry can be approximated using cubic spline interpolation of the coefficients A, B, C and D of varying crack lengths. This approach, demonstrated on the calculation of stress intensity factors for single edge crack geometry, resulted in a total loss of accuracy of less than 1%.

## INTRODUCTION

The importance of using fracture mechanics techniques in the structural design to account for the presence of crack has increased considerably over recent years. Linear elastic fracture mechanics analysis forms the basis for predicting the residual strength fatigue life of a cracked structure. The materials crack growth rate (da/dN) can be related to the cyclic changes in the stress intensity factor (ΔK). The stress intensity factor (K) embodies the effects of stress field, crack size, and structural geometry. Considerable efforts have been devoted to the computation of the stress intensity factors of complex geometries and loading. The versatile finite element method is well suited for computing the stress intensity factors of actual cracked structures of more complex stress/geometry combinations than those of comprehensive handbook solutions. (1,2)

By applying the well-known linear superposition method, a cracked structure subjected to remote loading can be replaced by the sum of (1) the uncracked stress analysis and (2) the cracked structure loaded with crack-face pressure loading, $\sigma(r_s)$, which is equal to and opposite the uncracked stress field that would exist at the crack-face. In other words, this linear superposition implies that the calculation of stress intensity factors under crack-face pressure loading $\sigma(r_s)$ is equivalent to loading the cracked body with remote loads that produce $\sigma(r_s)$ on the prospective crack face in the absence of a crack.

Rice (3) has shown that if both the displacement field and the stress intensity factors are known as a function of crack length for any symmetrical loading system acting on a linear elastic system, the stress intensity factor for any other symmetrical loading system of the same body can be determined using Bueckner's (4) weight function concept. These weight

functions are, in fact, the Green's function for the stress intensity factors in a cracked body. The weight function $h(x,y,a)$ is defined as:

$$h(a,x,y) = \frac{H}{K_I^*} \cdot \frac{\partial u^*(a,x,y)}{\partial a} \qquad (1)$$

where $H$ = effective modulus
$H = E$ for generalized plane stress state
$H = E/(1-\nu^2)$ for plane strain
$E$ = Young's modulus
$\nu$ = Poisson's ratio
$\frac{\partial u^*}{\partial a}$ = Derivative of displacement with respect to crack extension under * loading system.
and $K_I^*$ = Mode I stress intensity factor for * loading system.

The weight functions are defined for all locations within the structure. However, only the weight functions along the prospective crack face are of primary interest when evaluating the stress intensity factor with the intended approach. By employing the linear superposition principle, the efficient evaluation of stress intensity factors can be made by combining the equivalent uncracked crack-face pressure with the nodal weight functions along the crack face. Assume the crack-face nodal weight functions are designated as $h(a,r_s)$ for a given crack length a, where $r_s$ = distance from the crack-tip along the crack face.

Once the weight functions $h(a,r_s)$ have been determined for a given geometry, then K can be calculated for any crack size and shape from the uncracked stress field, $\sigma(r_s)$, on the prospective crack loci by:

$$K_I = \int_0^a dK_I(r_s) = \int_0^a h(a,r_s)\sigma(r_s)dr_s \qquad (2)$$

In a finite element analysis the "uncracked" stress field, $\sigma(r_s)$, on the prospective crack plane is replaced by N discretized consistent nodal tractions, $(f_1, f_2 \ldots f_n)$, as shown in the Appendix, for singular and non-singular quadratic isoparametric elements. Then the stress intensity factor for a given crack length, a, is obtained numerically by:

$$K_I(a) = \sum_{i=1}^{n} K_i(a) = \sum_{i=1}^{n} h_i(a,r_s)\, f_i \qquad (3)$$

where $K_i(a)$ = contribution from ith node to stress intensity factor

$f_i$ = equivalent nodal traction at ith node to represent "uncracked" pressure loading

and $h_i(a,r_s)$ = nodal weight function at ith nodal location.

Conceivably, the nodal weight functions, which depend on geometry only, can be accurately obtained from Eq. (1) with finite element analyses from a relatively simple loading condition and applied to complex stress fields. For the practical application of fracture mechanics, the evaluation of weight functions is often preferable to the calculation of stress intensity factors due to the load independent characteristics of weight functions. The application of finite element techniques to nodal weight function evaluation without using the singular elements has been recently demonstrated by Parks, et al (5), Vanderglas (6), and Vainshtok (7) using the virtual crack extension (VCE) method proposed by Parks (8) and Hellen (9). The virtual crack extension is a devised algorithm for the efficient calculation of the strain energy release rate (G) of a cracked structure. By evaluating the changes in global stiffness (K) and the prescribed nodal loads (f) for two slightly different crack lengths, the strain energy release rate can be evaluated. Pian, et al (10), have shown that the most accurate finite element scheme for determining the stress intensity factor uses the strain energy release rate. As indicated in Eq. (1), the evaluation of nodal weight functions require both the stress intensity factor and the displacement derivatives with respect to the virtual crack extension. Any error in $K_I$ and/or $\frac{\partial u}{\partial a}$ determinations will be carried into the inaccuracy in weight function evaluations. The accuracy of nodal weight functions is enhanced in the present work by combining the singular elements with the stiffness derivative technique.

Hensnell, et al (11), and Barsoum (12) have demonstrated that the quarter-point singular isoparametric elements with square root displacement variation radiating from the crack-tip are useful in the finite element computation of stress intensity factors. The singular elements have many merits: they are simple to use, compatible with the surrounding quadratic isoparametric elements, and the rigid body motion and constant strains are included in the shape function to facilitate the computation of $K_I$ under body force loading and thermal loading respectively. The use of the stiffness derivative technique, coupled with quarter-point degenerated singular elements, permits very efficient finite element determination of both stress intensity factors and the nodal weight functions. This paper demonstrates that accurate stress intensity factors can be obtained from a relatively coarse finite element mesh by coupling the stiffness derivative technique with singular elements.

The determination of nodal weight functions, which depend on geometry only, requires the evaluation of displacement derivatives at the original nodal location prior to the virtual crack extension under a given loading condition. The displacement derivatives at the perturbed nodal locations for the entire finite element model can be efficiently approximated from the perturbations in the elemental stiffness matrix and the prescribed nodal forces of only a limited number of elements. Corrections are made to the displacement derivatives to account for the perturbation of the nodal locations relative to the original nodal coordinates. This restores the characteristic $1/\sqrt{r}$ singular behavior to the nodal weight functions in the crack-tip neighborhood. The load independent characteristics of nodal weight functions are numerically demonstrated for a 2-D single edge crack under various remote loading and crack-face loading conditions. The load-independent property of weight functions has been rigorously proved by Rice (3).

The finite element method as suggested by Paris, et al (18) for weight function determination is obtained by inserting a small hole at the crack tip with Bueckner's $1/\sqrt{r}$ displacement singularity (4) as the boundary conditions on the hole to achieve the bounded energy. It is noted that with Bueckner's displacement singularity on the hole, the weight functions are actually contained in the computed dis-

placement field, as shown in Eq. (17) of Reference (18). On the other hand, the finite element method, as suggested by this paper for nodal weight function determination with singular elements, is achieved with Rice's definition (3) of weight function as shown in Eq. (1). Therefore $1/\sqrt{r}$ singularity for nodal weight functions is achieved with both finite element methods. In addition to the computational efficiency, the suggested method for weight function determination with singular elements can provide better accuracy near the crack tip than that of Paris, et al (18), by eliminating the small hole at the crack tip in dealing with a finite body.

Using the nodal weight function concept, the determination of the stress intensity factor is reduced to:

(1) Determination of the uncracked stress field
(2) Integration of Eq. (2) or (3) for appropriate geometry

In order to facilitate the utilization of the discretized nodal weight functions to determine $K_I$ using various mesh discretization of a selected geometry, the least-square fitting of both the near-field and far-field $h(a,r_s)$ values is employed:

$$h(a,r_s) = \frac{A(a)}{\sqrt{r_s}} + B(a) + C(a)\sqrt{r_s} + D(a)\, r_s \qquad (4)$$

where $r_s$ = radial distance from the crack-tip along crack-face. A, B, C, and D are coefficients of least-square fitting and are expressed as functions of crack size, (a).

Expressing the above coefficients as a function of crack length permits the interpolation of coefficients for the crack-face nodal weight functions at varying crack lengths. A cubic spline fitting method was successfully used to perform the required interpolation of the coefficients to evaluate the stress intensity factor at any crack length. As a result, a marked reduction in stress analyses is achieved through the use of the weight function concept to calculate the stress intensity factors of a structural component for predicting fatigue crack propagation life.

## FORMULATION

The finite element idealization of a 2-D crack geometry with uniform thickness was modeled with the degenerated quarter-point quadratic isoparametric elements with $\sqrt{r}$ displacement variation at the crack-tip vicinity. The singular crack-tip elements were surrounded by the standard 8-noded quadratic elements for the remainder of the 2-D model. A virtual crack extension of an amount $\Delta a$ of a Mode I crack was simulated by advancing the crack-tip node by $\Delta a$ in a "head-on" direction. The surrounding "quarter-point" nodes were also shifted to the new quarter-point locations. All other nodes in the model remain in their original positions. The other possible modes of virtual crack extension involve different zones of rigid body translation surrounding the crack-tip node. The virtual crack extension of the proposed mode, which is obtained by shrinking the zone of rigid body translation to a point at the crack-tip location, involves minimum computations.

The potential energy, $\pi$, of the finite element solution can be expressed as:

$$\pi = \frac{1}{2}\{u\}^T [K] \{u\} - \{u\}^T \{f\} \qquad (5)$$

where $\{u\}$ = displacement vector
$[K]$ = global stiffness matrix
$\{f\}$ = prescribed load vector
$\{u\}^T$ = transpose of $\{u\}$

It follows that the change in potential energy in a given loading geometry system produced by the virtual crack extension may be related to the strain energy release rate, G, as

$$G = -\left.\frac{\partial \Pi}{\partial a}\right|_{LOAD} = -\frac{1}{2}\{u\}^T \frac{\partial [K]}{\partial a}\{u\} + \{u\}^T \frac{\partial \{f\}}{\partial a} \qquad (6)$$

Since the stress intensity factor $K_I$ is related to G by

$$GH = K_I^2 \qquad (7)$$

where H = effective modulus

$K_I$ can be expressed as

$$K_I = \left\{\frac{1}{H}\left[-\frac{1}{2}\{u\}^T \frac{\partial [K]}{\partial a}\{u\} + \{u\}^T \frac{\partial \{f\}}{\partial a}\right]\right\}^{\frac{1}{2}} \qquad (8)$$

The global stiffness, $[K]$, which is the sum over all elemental stiffness $[k_i]$, depends on the individual elemental geometry, shape function, and elastic properties. In the proposed method of virtual crack extension, the degenerated crack-tip elements are the only elements in the 2-D model experiencing the changes in stiffness, $\frac{\partial [K]}{\partial a}$. Thus these elements comprise the evaluation of $\frac{\partial [K]}{\partial a}$. If there are $N_C$ crack-tip elements, the stiffness derivative becomes:

$$\frac{\partial [K]}{\partial a} = \sum_{i=1}^{N_C} \frac{\partial [k_i]}{\partial a} \qquad (9)$$

$[k_i]$ is the elemental stiffness of the ith element and $\frac{\partial [k_i]}{\partial a}$ can be approximated by simple finite differences as

$$\frac{\partial [k_i]}{\partial a} = \frac{[k_i]\big|_{a+\Delta a} - [k_i]\big|_a}{\Delta a} \qquad (10)$$

where

$[k_i]\big|_{a+\Delta a}$ = elemental stiffness after virtual crack extension

$[k_i]\big|_a$ = elemental stiffness before virtual crack extension

Similarly the $\frac{\partial \{f\}}{\partial a}$ can be approximated by finite differences as

$$\frac{\partial \{f\}}{\partial a} = \frac{\{f\}\big|_{a+\Delta a} - \{f\}\big|_a}{\Delta a} \qquad (11)$$

where $\{f\}\big|_{a+\Delta a}$ = consistent load vector after virtual crack extension

$\{f\}\big|_a$ = consistent load vector before virtual crack extension

$\frac{\partial\{f\}}{\partial a} \neq 0$. whenever body forces, thermal loading, and/or crack-face loading are applied. Only the crack-face ele ments with the perturbed nodal locations ($N_f$ of them) are involved in the numerical evaluation of $\frac{\partial\{f\}}{\partial a}$ :

$$\frac{\partial\{f\}}{\partial a} = \sum_{i=1}^{N_f} \frac{\{f_i\}|_{a+\Delta a} - \{f_i\}|_a}{\Delta a} \qquad (12)$$

$N_f$=1 is for the suggested approach for virtual crack extension. However, when surface tractions are applied on other than the crack-face element and there is no thermal loading or body force loading, then we have $\frac{\partial\{f\}}{\partial a} = 0$. Thus, Eq. (6) is simplified to

$$G = -\frac{1}{2}\{u\}^T \frac{\partial[K]}{\partial a}\{u\} \qquad (13)$$

Since the evaluation of $\frac{\partial[K]}{\partial a}$ and $\frac{\partial\{f\}}{\partial a}$ involves only a few elements, the numerical calculation of strain energy release rate ($G = -\frac{\partial\pi}{\partial a}$) can be efficiently made by adopting the virtual crack extension approach.

The evaluation of the nodal weight function h(a,x,y), as indicated in Eq. (1), requires the calculation of both the stress intensity factor ($K_I$) and the displacement derivatives, $\frac{\partial u}{\partial a}$ at the unperturbed nodal locations. However, the displacement derivative at the perturbed nodal locations, $\frac{du}{da}$, can be derived from the global stiffness equation of

$$[K]\{u\} = \{f\} \qquad (14)$$

By differentiating Eq. (14) with respect to the crack length (a)

$$[K]\frac{d\{u\}}{da} + \frac{d[K]}{da}\{u\} = \frac{d\{f\}}{da} \qquad (15)$$

After rearranging we have

$$\frac{d\{u\}}{da} = [K]^{-1}\left[\frac{d\{f\}}{da} - \frac{d[K]}{da}\{u\}\right] \qquad (16)$$

Eq. (16) indicates that the displacement derivatives, with reference to the perturbed nodal locations for the whole structure, can be obtained from the perturbation in stiffness and prescribed nodal forces of a few elements. The $\frac{d\{f\}}{da}$ term of Eq. (16) must be taken into account when dealing with crack-face loading, thermal loading, and body force loading conditions. The numerical results of this paper verify that in evaluating the stress intensity factor and nodal weight functions, the crack-face loading $\sigma(r_s)$ is equivalent to loading the same cracked geometry with loads that produce $\sigma(r_s)$ on the prospective crack face in the absence of a crack.

The $\frac{d[K]}{da}\{u\}$ term in Eq. (16) resembles a "pseudo-force" vector-per-unit crack extension. The numerical evaluation of displacement derivatives at the perturbed nodal locations for the whole structure can be economically achieved from the changes in $\frac{d\{f\}}{da}$ and $\frac{d[K]}{da}$. Since only a few elements involve an actual change in stiffness and in prescribed consistent nodal traction, the evaluation of displacement derivatives of Eq. (16) is relatively inexpensive for the virtually extended crack geometry. The nodal weight functions of Eq. (1) require the displacement derivative with respect to the crack extension in original coordinates. However, the displacement derivatives obtained from Eq. (16) are referenced to the updated geometry. The numerical corrections for the displacement derivatives from the updated geometry to the original coordinates, as suggested by Vanderglas (14), are as follows:

The displacement field is expressed as;

$$u = u\ (x,y,a) \qquad (17)$$

Applying chain rule and differentiating with respect to flaw size, (a)

$$\frac{d\{u\}}{da} = \frac{\partial\{u\}}{\partial x}\cdot\frac{dx}{da} + \frac{\partial\{u\}}{\partial y}\cdot\frac{dy}{da} + \frac{\partial\{u\}}{\partial a} \qquad (18)$$

Rearranging Eq. (18)

$$\frac{\partial\{u\}}{\partial a} = \frac{d\{u\}}{da} - \frac{\partial\{u\}}{\partial x}\cdot\frac{dx}{da} - \frac{\partial\{u\}}{\partial y}\cdot\frac{dy}{da} \qquad (19)$$

For isoparametric elements, the elemental displacement, u, can be expressed as

$$u = N_i\, u_i \qquad (20)$$

where $N_i$ = shape function
$u_i$ = nodal displacement

To facilitate the evaluation of $\frac{\partial\{u\}}{\partial x}$ and $\frac{\partial\{u\}}{\partial y}$ in Eq. (19), the mapping between local coordinates ($\xi,\zeta$) and global coordinates (x,y) is made per the following equations;

$$\frac{\partial\{u\}}{\partial x} = \frac{1}{\det[J]}\left\{\frac{\partial[N_i u_i]}{\partial\xi}\cdot\frac{\partial y}{\partial\zeta} - \frac{\partial[N_i u_i]}{\partial\zeta}\cdot\frac{\partial y}{\partial\xi}\right\} \qquad (21a)$$

$$\frac{\partial\{u\}}{\partial y} = \frac{1}{\det[J]}\left\{\frac{\partial[N_i u_i]}{\partial\zeta}\cdot\frac{\partial x}{\partial\xi} - \frac{\partial[N_i u_i]}{\partial\xi}\cdot\frac{\partial x}{\partial\zeta}\right\} \qquad (21b)$$

where [J] = Jacobian matrix
and det [J] = determinant of [J]

By substituting Eq. (21) into (19), the displacement derivatives in original coordinates can be expressed as:

$$\frac{\partial\{u\}}{\partial a} = \left[\frac{d\{u\}}{da} - \frac{1}{\det[J]}\left\{\frac{\partial[N_i u_i]}{\partial\xi}\cdot\frac{\partial y}{\partial\zeta} - \frac{\partial[N_i u_i]}{\partial\zeta}\cdot\frac{\partial y}{\partial\xi}\right\}\frac{dx}{da}\right] - \frac{1}{\det[J]}\left\{\frac{\partial[N_i u_i]}{\partial\zeta}\cdot\frac{\partial x}{\partial\xi} - \frac{\partial[N_i u_i]}{\partial\xi}\cdot\frac{\partial x}{\partial\zeta}\right\}\frac{dy}{da} \qquad (22)$$

For "head on" crack extension of a Mode I crack, we have $\frac{dx}{da} = 1.0$ and $\frac{dy}{da} = 0.0$. Therefore, Eq. (22) becomes:

$$\frac{\partial\{u\}}{\partial a} = \left[\frac{d\{u\}}{da} - \frac{1}{\det[J]}\left\{\frac{\partial[N_i u_i]}{\partial\xi}\cdot\frac{\partial y}{\partial\zeta} - \frac{\partial[N_i u_i]}{\partial\zeta}\cdot\frac{\partial y}{\partial\xi}\right\}\right] \qquad (23)$$

Substituting Eq. (23) into (1), the nodal weight function can be expressed as:

$$h_i(a,x,y) = \frac{H}{K_I}\left[\frac{d\{u\}}{da} - \frac{1}{\det[J]}\left\{\frac{\partial[N_i u_i]}{\partial\xi}\cdot\frac{\partial y}{\partial\zeta} - \frac{\partial[N_i u_i]}{\partial\zeta}\cdot\frac{\partial y}{\partial\xi}\right\}\right] \qquad (24)$$

As indicated in Fig. 6, the $1/\sqrt{r}$ singular behavior of the nodal weight functions in the crack-tip neighborhood is duly restored after the coordinate transformation corrections are made for the displacement derivatives.

Normally, the finite element evaluation of stress intensity factor using strain energy release rate requires two successive analyses of slightly different crack sizes. By adopting the technique of virtual crack extension, the calculation of strain energy changes can be accomplished with the finite element solution of the original crack configuration and the additional analysis of a few elements with perturbed nodal locations. The calculation of nodal weight functions for a given geometry requires both the stress intensity factor and the displacement derivatives under a given loading system. By incorporating the singular elements into the stiffness derivative technique, accuracy enhancement is achieved for both the stress intensity factors and the displacement derivatives. The application of singularity elements to the stiffness derivative technique of Parks (8) and Hellen (9) provides the most efficient finite element calculation for both the stress intensity factors and the nodal weight functions.

## RESULTS AND DISCUSSIONS

The enhancement of solution accuracy for both stress intensity factors and nodal weight functions is achieved by applying the singularity elements to the stiffness derivative technique. By applying the linear superposition principle, the evaluation of stress intensity factors and nodal weight functions of a cracked body can be obtained using the equivalent "uncracked" crack-face loading to replace the remote loading. This equivalency is verified numerically by taking account of $\frac{\partial(f)}{\partial a}$ term in evaluating the changes in potential energy and displacement derivatives. The evaluation of the displacement derivatives for nodal weight function calculation requires the adjustment from the perturbed nodal location to the original positions for the perturbed nodes. After the adjustments are made, the $1/\sqrt{r}$ singular behavior in the vicinity of crack-tip is duly restored. An engineering approach is proposed to express both the near-field and far-field crack-face nodal weight functions as a function of distance from the crack-tip for a given crack length. This approach allows the efficient evaluation of crack-face nodal weight functions at any crack length.

One of the key operational parameters for the stiffness derivative technique is the incremental crack size ($\Delta a$) associated with the virtual crack extension. A relatively coarse mesh (as shown in Fig. 1a) of the single edge crack specimen under generalized plane stress state with $\frac{a}{w} = 0.5$, $\frac{H}{w} = 3.0$ and $\frac{\ell_s}{a} = 0.3$ was used to study the solution stability. Both the stress intensity factors and the nodal weight functions are stable over a wide range of $10^{-13} \leq \Delta a/\ell_s \leq 10^{-3}$ ratio. The plot of normalized $K_I/\sigma\sqrt{\pi a}$ value as a function of $\frac{\Delta a}{\ell_s}$ ratio is shown in Fig. 2. When $\Delta a/\ell_s \geq 10^{-3}$, the solution deterioration is observed due to the excessive shape distortion of the degenerated crack-tip elements as a result of virtual crack extension. When $\Delta a/\ell_s \leq 10^{-13}$, the solution degradation is also observed, due mainly to the round-off error of geometric input data being carried into finite element computations.

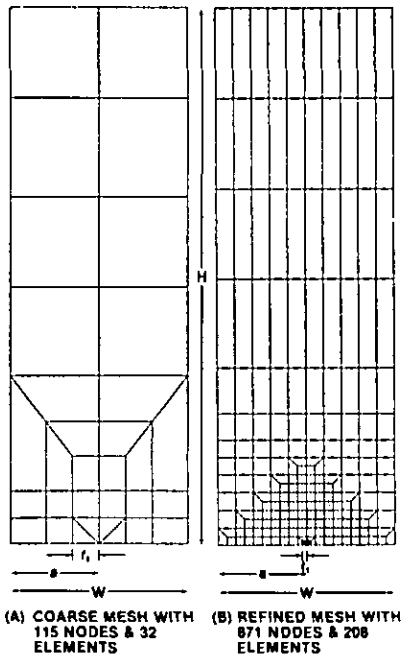


Fig. 1. 2-D Mesh Idealizations used for Modeling the Single Edge Crack (Sec) Specimen.

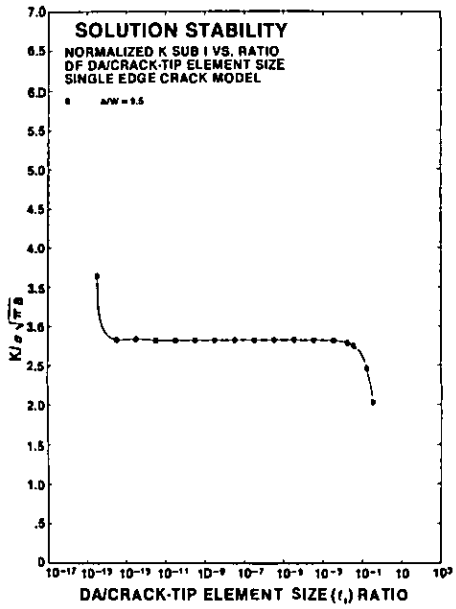


Fig. 2. Effect of Incremental Crack Size ($\Delta a$) of Virtual Crack Extension on Solution Stability; $K_I/\sigma\sqrt{\pi a}$ vs. $\Delta a / \ell_s$ ratios.

All geometric input and numerical computations were made using double precision on a IBM machine in our finite element implementation of stiffness derivative technique. It appears that the $K_I$ solutions approach the converged $K_I$ value as $\Delta a/\ell_s$ ratio decreases before showing accuracy degradation due to the round-off error. For practical purposes, $\frac{\Delta a}{\ell_s}$ ratio value of $10^{-5}$, which is used to generate the numerical results reported in this paper, is sufficient to ensure the solution stability.

The advantage of applying the degenerated quarter-point singular elements in the immediate crack-tip vicinity to the stiffness derivative technique is convincingly shown in Fig. 3, especially for relatively coarse finite element mesh. Fig. 3 shows the normalized $K_I/\sigma\sqrt{\pi a}$ as a function of $\ell_s/a$ ratio with different mesh refinements for a single edge crack geometry of $\frac{a}{w} = 0.5$ and $\frac{H}{w} = 3.0$ subjected to remote tension loading ($\sigma$). These results suggest that by coupling the singularity elements with the stiffness derivative technique, stress intensity factors with less than 1% error can be obtained with a relatively coarse mesh. As suggested by Ingraffea, et al (15), and Shih, et al (16), the stress intensity factors can also be calculated from the crack opening displacements of the singular crack-tip element along the crack face. For the generalized plane stress problem, $K_I$ is related to the crack opening displacements (COD) by

$$K_I = \frac{E\sqrt{2\pi}}{4}\left[\frac{4V_B - V_C}{\sqrt{\ell_s}}\right] \qquad (25)$$

where $V_B$ = COD at quarter-node location
and $V_C$ = COD at corner node location

Results in the present study indicate that the convergence rate is faster when the $K_I$ value is obtained with the stiffness derivative technique rather than with the use of Eq. (25) with crack opening displacements of singular elements. For example, the ratio of $K_I/\sigma\sqrt{\pi a} = 2.818$ was obtained from the stiffness derivative technique with $\frac{\Delta a}{\ell_s} = 10^{-5}$ for the single edge crack of $\frac{a}{w} = 0.5$ and $\frac{H}{w} = 3.0$ with coarse mesh, as shown in Fig. 1a. On the contrary, $K_I/\sigma\sqrt{\pi a} = 2.685$ was obtained from Eq. (25) with crack opening displacement of singular crack-tip element. Gross, et al (17), obtained a numerical value of $K_I/\sigma\sqrt{\pi a} = 2.82$. If this solution is adopted as the reference, a relative error of less than 0.1% will be obtained from using the stiffness derivative technique, in contrast to a 4.8% error when using Eq. (25).

The normalized nodal weight functions, $n(a,r)\sqrt{w}$, for the single edge crack specimen with $\frac{a}{w} = 0.5$ as a function of normalized distance along the top "remote loading face" and along the crack face with and without singular elements, are shown in Fig. 4 and Fig. 5 respectively. The resulting nodal weight functions obtained with singularity elements compare favorably with that of Paris, et al (18). As indicated in Fig. 4, the nodal weight function along the "top-face" is relatively insensitive to the mesh refinment. The accuracy of the singular behavior for the crack-face nodal weight functions in crack-tip neighborhood can potentially suffer with the use of a relatively coarse mesh. It was found that by employing Eq. (4) to describe the near-field and far-field approximation, an

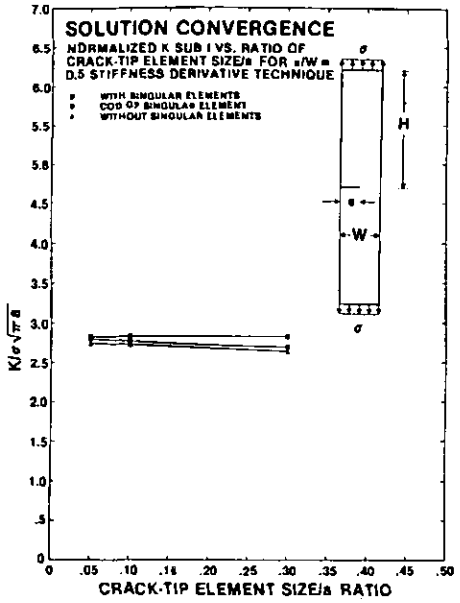


Fig. 3. Dependence of $K_I$ Solution Accuracy on Crack-Face Element Size ($\ell_s$).

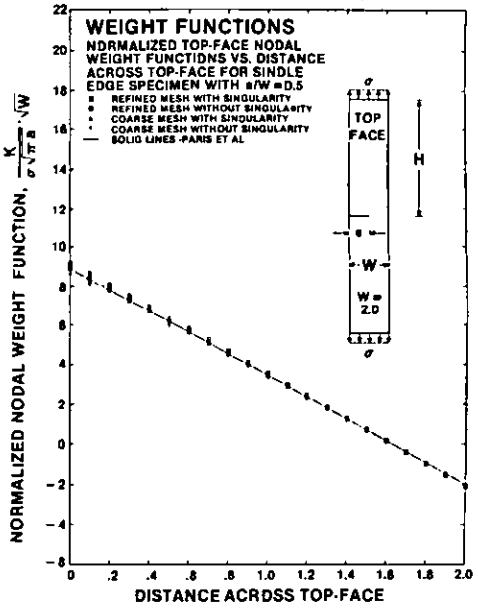


Fig. 4. Normalized Nodal Weight Functions Across the Top-Face for Single Edge Crack Geometry with $\frac{a}{w} = 0.5$.

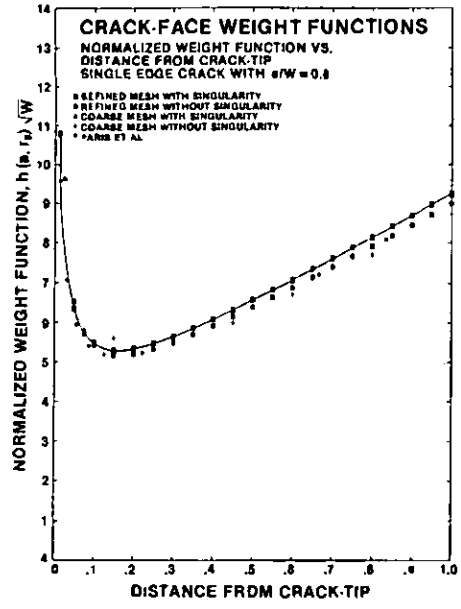


Fig. 5. Normalized Crack-Face Nodal Weight Functions as a Function of Distance from Crack-Tip with and without Singular Elements for Sec Specimen with $\frac{a}{w} = 0.5$.

accurate representation of nodal weight functions along the entire crack face can be obtained from a relatively coarse mesh, as shown in Fig. 6. The bulk of the data reported was obtained using refined meshes of varying crack lengths, similar to that of Fig. 1b, for the convenience of obtaining nodal weight functions with range of $\frac{a}{w}$ ratios. As indicated in Fig. 5, the application of singular elements to the stiffness derivative technique can improve the accuracy of crack-face nodal weight functions. This resulted from the increased accuracy in the $K_I$ and $\frac{\partial\{u\}}{\partial a}$ determinations. The data points, which fall well below the $1/\sqrt{r}$ singular behavior of nodal weight function in crack-tip neighborhood, as shown in Fig. 5, are obtained without taking into account the coordinate perturbation of displacement derivatives of the virtually displaced nodes for coarse mesh and refined mesh with singular crack-tip elements. After the coordinate corrections are made according to Eq. (19) for displacement derivatives, the $1/\sqrt{r}$ singular behavior of the nodal weight functions is duly restored in the crack-tip neighborhood.

It appears that coupling the stiffness derivative technique with singularity elements provides an efficient finite element scheme that can be used to determine both stress intensity factors and nodal weight functions.

The load independent characteristic of nodal weight functions for a given crack geometry were numerically verified with single edge crack geometry with $\frac{a}{w}$ = 0.3, 0.5, and 0.7 subjected to remote tension and the equivalent crack-face tension conditions. These verification efforts are intended to achieve the economic evaluation of accurate stress intensity factors by combining the consistent nodal tractions to represent the "uncracked" stress field with the predetermined nodal weight functions along the crack face, according to Eq. (3), without involving stress analysis of cracked body. Consequently, major attention is focused, as indicated in this paper, on facilitating the utilization of crack-face nodal weight functions, $h(a,r_s)$, for accurate evaluation of stress intensity factors.

From a computational viewpoint, the different procedures are involved in evaluating both the stress intensity factors and the nodal weight functions by replacing the problem of the cracked body subjected to complex loading condition, including thermal and body force loadings with the equivalent "uncracked" crack-face loading based on the superposition principle. Whenever involving crack-face loading, the numerical evaluation of potential energy changes, as shown in Eq. (6), requires the inclusion of $\frac{\partial\{f\}}{\partial a}$ term in addition to $1/2\ \{u\}\frac{\partial[K]}{\partial a}\{u\}$ term. However, the $\frac{\partial\{f\}}{\partial a}$ term becomes null for virtual crack extension when a cracked body is subjected to remote loading only. Also, the computation of the displacement derivative at the perturbed nodal location for the weight function evaluation shown in Eq. (16) needs to take $\frac{\partial\{f\}}{\partial a}$ term into consideration whenever crack-face loading is applied. After taking $\frac{\partial\{f\}}{\partial a}$ into account in Eq. (6) and (16), the equivalence between the remote loading and the corresponding crack-face loading for $K_I$ and $h(a,x,y)$ equations is achieved within the numerically acceptable accuracy for both stress intensity factors and nodal weight functions between the remote loading condition and the equivalent crack-face loading case.

Prior literature did not account for the $\frac{\partial\{f\}}{\partial a}$ term in the numerical computation of nodal weight functions. This was not a subject of investigation, since crack-face loading was not part of prior solutions. The nodal weight functions as a function of distance from crack-tip along crack face are shown in Fig. 7 for the single edge crack model with $\frac{a}{w}$ = 0.3, 0.5, and 0.7 subjected to crack-face tension. The corresponding case with remote tension condition is shown along with that of the crack-face loading cases. Favorable agreement is exhibited between the two sets

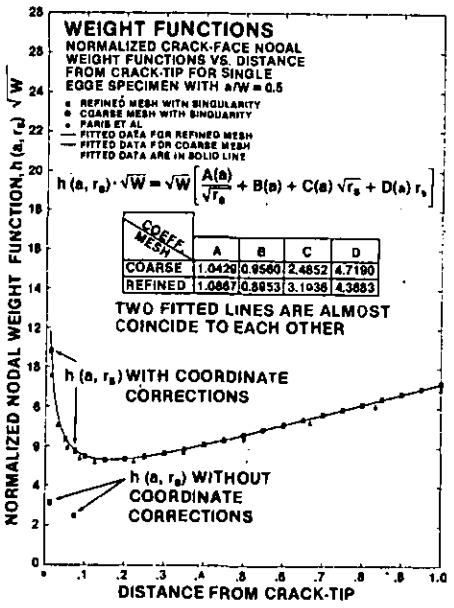


Fig. 6. Comparison Between Fitted and Calculated Crack-Face Nodal Weight Functions for Sec Specimen of $\frac{a}{w}$ = 0.5 with Coarse and Refined Meshes.

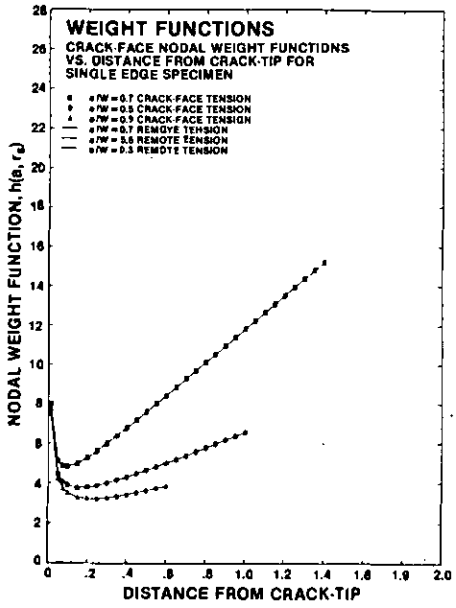


Fig. 7. Compare Crack-Face Nodal Weight Functions obtained from the Remote Load and Equivalent Crack-Face Loading Conditions for Sec Specimen.

of data. A maximum difference of less than 0.01% in the crack-face nodal weight function is seen between the crack-face loading condition and the equivalent remote loading case.

It is noted that the equivalent nodal tractions representing a pressure distribution on a given face of the quarter-point singular element differs drastically from that of the regular 8-noded quadratic isoparametric element. For a regular quadratic isoparametric element, the nodal tractions for uniform pressure are represented by 1/6, 4/6, 1/6 of total pressure force. The 4/6 is applied to the midside node. The consistent nodal tractions for the same uniform pressure are represented for singular elements by 1/3, 2/3, and 0 of total pressure forces, with 1/3 for corner node far away from crack-tip node, 2/3 for quarter-point node, and 0 for crack-tip node. The derivation of the consistent nodal force representation for a given pressure distribution on singular elements is shown in the Appendix. In dealing with non-uniform crack-face loading, the finite element implementation of the stiffness derivative technique requires the calculation of the equivalent consistent nodal tractions at the perturbed and discretized nodal locations to reflect the localized pressure change on the crack face as a result of the virtual crack extension.

In order to facilitate calculation of $K_I$ for life prediction purposes, $K_I$ must be evaluated for any crack size from Eq. (3) by coupling the "uncracked" stress field with the predetermined crack-face nodal weight functions of varying crack lengths without involving stress analysis of cracked body. This approach requires the accurate near-field and far-field representation of crack-face nodal weight functions for each given crack geometry. By applying an accurate interpolative capability to the existing nodal weight functions of varying crack lengths, the crack-face nodal weight functions of any crack size can be determined.

By using least-squares procedures, the discretized values of near-field and far-field crack-face nodal weight functions, $h(a,r_s)$, of any individual crack length (a) are approximated successfully with Eq. (4). This selection of Eq. (4) is based on the fact that the weight function definition shown in Eq. (1) is proportional to the derivatives of displacement field. It is known that the displacement field of a cracked body is in the form of infinite power series of $\sqrt{r}$. Terms higher than $r^2$ were not required since the numerical results indicated that the far-field nodal weight functions in a linear fashion.

Cubic spline fitting procedures were applied and used to interpolate the coefficients A, B, C, and D of Eq. (4) for other crack lengths. By coupling the "uncracked" stress field with the interpolated crack-face nodal weight functions, $h(a,r_s)$, the accurate stress intensity factors can be obtained without involving stress analysis of the cracked structure.

This suggested procedure to evaluate the $K_I$ value of any crack size from the "uncracked" stress field and the interpolated $h(a,r_s)$ values along the crack face are demonstrated in this paper with single edge crack geometry. Fig. 8 shows the comparison between the actual nodal weight function data, which are obtained from finite element analysis with application of singular elements to stiffness derivative technique, and the fitted nodal weight functions, which are calculated from the coefficients A, B, C, and D of Eq. (4). These nodal weight functions for $\frac{a}{w}$ = 0.2, 0.3, 0.5, 0.6, 0.7, 0.8 are well represented by Eq. (4). The maximum error between the actual and fitted weight function is found to be less than 1%. The tabulation of the coefficients A, B, C, and D for single edge crack geometry is shown in Table 1.

Table I
Least-Square Coefficients of Equation (4) for Single Edge Crack Geometry with $\frac{H}{W}$ = 3.0

| Coeff. Ratio | A | B | C | D |
|---|---|---|---|---|
| 0.2 | 0.79759 | 0.05833 | 2.10402 | 1.83560 |
| 0.3 | 0.79264 | 0.13116 | 2.12559 | 1.75033 |
| 0.4 | 0.77957 | 0.29202 | 2.07923 | 2.27180 |
| 0.5 | 0.76838 | 0.42092 | 2.25819 | 3.08956 |
| 0.6 | 0.74347 | 0.72122 | 2.21545 | 4.70897 |
| 0.7 | 0.70919 | 1.11847 | 2.30360 | 7.69152 |
| 0.8 | 0.64092 | 1.96383 | 2.13187 | 14.90447 |

The interpolated crack-face nodal weight functions for an arbitrary crack length have been determined with the use of a cubic spline fitting of the $h(a,r_s)$ data with $\frac{a}{w}$ = 0.2, 0.3, 0.5, 0.6, 0.7, and 0.8. The accuracy of the predicted nodal weight functions for $\frac{a}{w}$ = 0.45, 0.55, and 0.65 were checked directly against the direct finite element results shown in Fig. 9. The maximum error is found to be less than 0.5%. By combining the "uncracked" stress field with the interpolated nodal weight functions, the accurate stress intensity can be economically estimated according to Eq. (3). The error of the predicted $K_I$ data is found to be less than 1.0% for the demonstration problem of single edge crack geometry.

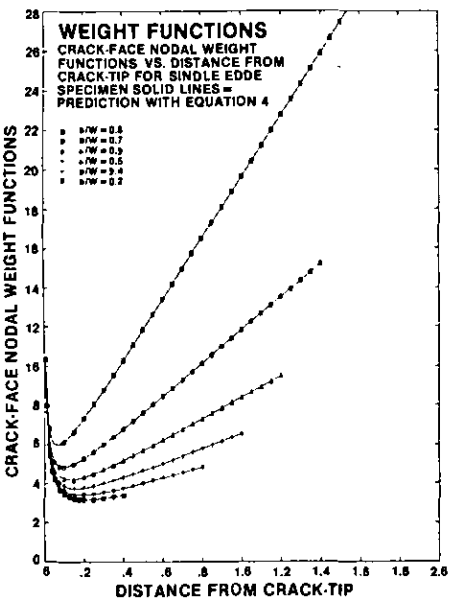


Fig. 8. Comparison between Fitted and Calculated Crack-Face Nodal Weight Functions as a Function of Crack-Face Distance for Sec Specimen with different $\frac{a}{w}$ ratios.

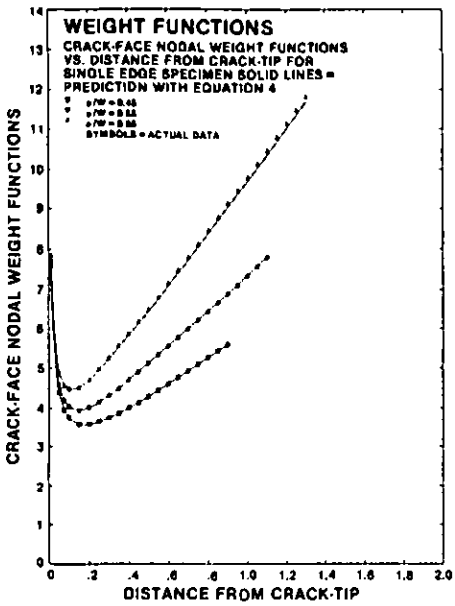


Fig. 9. Comparison Between the Calculated and the Predicted Crack-Face Nodal Weight Functions of Sec Specimen with Different $\frac{a}{w}$ ratios.

## CONCLUSIONS

- The application of singular crack-tip elements to the stiffness derivative technique can enhance the accuracy in determining the stress intensity factors and nodal weight functions. The accuracy improvement of nodal weight functions with singularity elements is due to the reduced error of $K_I$ and $\frac{\partial\{u\}}{\partial a}$ determinations.
- In applying fracture mechanics to a given component geometry, the weight-function evaluation is more favorable than that of the stress intensity factor calculation because of load independent characteristics of weight functions. The nodal weight function evaluation involves the additional computational effort of calculating the displacement derivatives with respect to the crack-tip coordinates. By coupling the singular crack-tip elements with the virtual crack extension method of Parks (8) and Hellen (9), an efficient finite element scheme is achieved.
- The principle of linear superposition implies that the determination of the stress intensity factors and crack-face nodal weight functions of a given geometry can be made by replacing the crack face loading $\sigma(r_s)$ with the far-field loads that produce the $\sigma(r_s)$ on the prospective crack face in the absence of a crack.
  Numerical demonstration of this equivalence requires the addition of the $\frac{\partial\{f_i\}}{\partial a}$ term in Eq. (6) and (16) in handling crack-face loading case to calculate the strain energy release rate and the displacement derivative respectively. The numerical accuracy was achieved to support the equivalency derived by the linear superposition principle.
- The correction of the perturbed coordinates to the original coordinates is required to evaluate the displacement derivatives used in the determination of nodal weight functions. After the correction is made, the required $1/\sqrt{r}$ singular behavior of the nodal weight functions in the immediate vicinity of crack-tip is restored.
- It is found that both the near-field and far-field nodal weight functions along the crack face can be accurately presented by

$$h(a,r_s) = \frac{A(a)}{\sqrt{r_s}} + B(a) + C(a)\sqrt{r_s} + D(a)\, r_s$$

  These coefficients A(a), B(a), C(a), and D(a), which are functions of crack length (a), can be determined by least-squares fitting procedures. An interpolation procedure using a cubic spline fitting technique is suggested to interpolate the nodal weight functions for other crack lengths. The single edge crack specimen results suggest that the total loss of accuracy of the calculated stress intensity factor from the nodal weight function with the proposed interpolation procedures is less than 1%.
- By using the linear superposition principle and the nodal weight function concept, the accurate stress intensity factor can be economically calculated from the uncracked stress field and the crack-face nodal weight functions without performing stress analyses of the cracked body. Therefore, a drastic reduction of stress analysis is accomplished through the use of weight function concepts to accurately calculate the stress intensity factors for predicting fatigue crack propagation life of a structural component.

## ACKNOWLEDGEMENT

The author wishes to thank Mr. Stacy E. Thompson, Supervisor of Design Automation of Detroit Diesel Allison, Division of General Motors Corporation, for his efforts in the implementation of stiffness derivative technique.

## REFERENCES

1. H. Tada, P. Paris and G. Irwin, "The Stress Analysis of Cracks Handbook," Del Research Corporation (1973).
2. G. C. Sih, "Handbook of Stress Intensity Factors," Institute of Fracture and Solid Mechanics, Lehigh University (1973).
3. J. R. Rice, "Some Remarks on Elastic Crack-Tip Stress Fields," International Journal Solids Structures, Vol. 8, 1972, pp 751-758.
4. H. F. Bueckner, "Field Singularities and Related Integral Representations," Mechanics of Fracture I, Method of Analysis and Solutions of Crack Problems, edited by G. C. Sih, Noordhooff International Publishing (1972).
5. D. M. Parks and E. M. Kamentzky, "Weight Functions from Virtual Crack Extension," International Journal for Numerical Method in Engineering, Vol. 14, (1979), pp 1693-1706.
6. M. L. Vanderglas, "Weight Functions for Plans and Axisymmetric Crack Problems," Numerical Methods in Fracture Mechanics, edited by D. R. J. Owen and A. R. Luxmoore, Pineridge Press., (1980) pp 51-65.

7. V. A. Vainshtok, "Virtual Crack Variation Method for Determination of Stress Intensity Factors for Cracks of Mixed Mode and Variable Length," Innovative Numerical Analysis for the Applied Engineering Sciences, University Press of Virginia, (1980) pp 797-803.

8. D. M. Parks, "A Stiffness Derivative Finite Element Technique for Determination of Crack Tip Stress Intensity Factors," International Journal of Fracture, Vol. 10, (1974), pp 487-501.

9. T. K. Hellen, "On the Method of Virtual Crack Extensions," International Journal for Numerical Methods in Engineering, Vol. 9, (1975), pp 187-207.

10. Pian Tong and T. H. H. Pian, "On the Convergence of the Finite Element Method for Problems with Singularity," International Journal Solids and Structures, Vol. 9, (1973), pp 313-321.

11. R. D. Henshell and K. G. Shaw, "Crack Tip Elements are Unnecessary," International Journal for Numerical Methods in Engineering, Vol. 9, (1975), pp 495-507.

12. R. S. Barsoum, "On the Use of Isoparametric Finite Elements in Linear Fracture Mechanics," International Journal of Numerical Methods Engineering, Vol. 10, (1976), pp 25-37.

13. O. C. Zienkiewicz, The Finite Element Method, Third Edition McGraw-Hill (1977).

14. M. L. Vanderglas, "A Stiffness Derivative Finite Element Technique for Determination of Influence Functions," International Journal of Fracture Vol. 14, (1978), pp 291-295.

15. A. R. Ingraffea and Corneliu Manu, "Stress Intensity Factor Computation in Three Dimensions with Quarter-Point Elements," International Journal for Numerical Methods in Engineering, Vol. 15, (1980), pp 1427-1445.

16. C. F. Shih, H. G. deLorenzi, and M. D. German, "Crack Extension Modeling with Singular Quadratic Isoparametric Elements," International Journal of Fracture, Vol. 12, (1976), pp 647-651.

17. B. Gross and J. E. Scowley, "Stress-Intensity Factors for a Single-Edge Notch Tension Specimen by Boundary Collocation of a Stress Function," NASA TN D-2395 (1964).

18. P. C. Paris, R. N. McMeeking, and H. Tada, "The Weight Function Method for Determining Stress Intensity Factors," ASTM STP 601, American Society for Testing and Materials, (1976), pp 471-489.

## APPENDIX

### Equivalent consistent nodal tractions for pressure loading.

By virtual work consideration, the equivalent consistent nodal tractions for pressure $\sigma$ applied on an infinitesimal area dA of real coordinates, which are mapped into the face of $\eta = -1$ and $-1 \leq \xi \leq 1$ of nature coordinates ($\xi$, $\eta$ ) of a 2-D quadratic element, takes the form of:

$$[f]^e = \int_A [N^e]^T \sigma(A) dA \qquad (A1)$$

where $[f]^e$ = elemental force vector
$[N^e]^T$ = transpose of shape function matrix

and dA = dx for unit thickness

The pressure can be any function of x. The linear variation of $\sigma(x) = \sigma_o + mx$ is assumed in the following discussion for illustration purposes. Mapping is made for three nodes i, j, and k in x-space with either $(x_i, x_j, x_k) = (0.0, 0.5, 1.0)$ for standard quadratic element or $(x_i, x_j, x_k) = (0.0, 0.75, 1.0)$ for singular quadratic element into nature coordinate $\xi$ such that $(\xi_i, \xi_j, \xi_k) = (-1, 0, 1)$. By changing the variable from x to $\xi$, Eq. (A1) becomes;

$$[f]^e = \int_{-1}^{+1} [N^e]^T \sigma(\xi) \det[J] \, d\xi \qquad (A2)$$

where $[N^e]^T = [N_i, N_j, N_k]$

$$N_i = -\frac{\xi}{2}(1 - \xi)$$

$$N_j = (1 + \xi)(1 - \xi)$$

$$N_k = \frac{\xi}{2}(1 + \xi)$$

and $[J]$ = Jacobian matrix $= \frac{dx}{d\xi} = \det[J]$

From the interpolating equation of isoparametric element, we have

$$X = \sum_{i=1}^{3} N_i X_i \qquad (A3)$$

where $X_i$ = nodal quantity at ith location in x-space

By substituting (A3) the into Jacobian matrix, we have

$$[J] = \frac{dN_i}{d\xi} X_i + \frac{dN_j}{d\xi} X_j + \frac{dN_k}{d\xi} X_k \qquad (A4)$$

For non-singular quadratic element with $(x_i, x_j, x_k) = (0.0, 0.5, 1.0)$, we have $[J] = 1/2$. For singular elements with $(x_i, x_j, x_k) = (0.0, 0.75, 1.0)$ and with kth node as crack-tip node we have $[J] = 1/2\,(1-\xi)$; which implies that

$[J] = 1$ at ith node
$[J] = 1/2$ at jth node
and $[J] = 0$ at kth node in x-space

The equivalent consistent nodal tractions, $f_i$, $f_j$, and $f_k$ can be calculated for $\sigma(x) = \sigma_o + mx$ as follows:

(A) for non-singular element

$$\sigma(x) = \sigma_o + mx$$
$$= \sigma_o + m\,(N_i X_i + N_j X_j + N_k X_k)$$

By substituting $N = N(\xi)$, and the values of $(x_i, x_j, x_k) = (0.0, 0.5, 1.0)$ we have

$$\sigma(\xi) = \sigma_o + m/2\,(1 + \xi) \qquad (A5)$$

By substituting (A5) and det |J| = 1/2 into (A2), we have

$$f_i = \int_{-1}^{+1} \left(\frac{-\xi}{2}\right)(1 - \xi)\left[\sigma_o + \frac{m}{2}(1+\xi)\right]\frac{1}{2}\, d\xi = \frac{\sigma_o}{6} \qquad (A6)$$

$$f_j = \int_{-1}^{+1} (1+\xi)(1-\xi)\left[\sigma_o + \frac{m}{2}(1+\xi)\right]\frac{1}{2}\, d\xi = \frac{2\sigma_o + m}{3} \qquad (A7)$$

$$f_k = \int_{-1}^{+1} \frac{\xi}{2}(1+\xi)\left[\sigma_o + \frac{m}{2}(1+\xi)\right]\frac{1}{2}\, d\xi = \frac{\sigma_o + m}{6} \qquad (A8)$$

(B) For singular element:

By substituting $\sigma(\xi)$ and det |J| = 1/2 (1 - $\xi$) into Eq. (A2), we have

$$f_i = \int_{-1}^{+1} \left(\frac{-\xi}{2}\right)(1-\xi)\left[\sigma_o + \frac{m}{2}(1+\xi)\right]\frac{1}{2}(1-\xi)\, d\xi = \frac{10\sigma_o + m}{30} \qquad (A9)$$

$$f_j = \int_{-1}^{+1} (1+\xi)(1-\xi)\left[\sigma_o + \frac{m}{2}(1+\xi)\right]\frac{1}{2}(1-\xi)\, d\xi = \frac{10\sigma_o - 4m}{15} \qquad (A10)$$

$$f_k = \int_{-1}^{+1} \frac{\xi}{2}(1+\xi)\left[\sigma_o + \frac{m}{2}(1+\xi)\right]\frac{1}{2}(1-\xi)\, d\xi = \frac{m}{30} \qquad (A11)$$

These results indicated that for a given pressure the consistent nodal tractions for singular elements differ drastically from that for regular quadratic elements. If uniform pressure is applied, we have $\sigma(x) = \sigma(\xi) = \sigma o$ and m = 0. From Eq. (A6), (A7), and (A8) for non-singular quadratic element, we have $f_i = \sigma_o/6$, $f_j = 2/3\ \sigma_o$, and $f_K = \sigma_o/6$, which are consistent with solutions provided by Zienkiewicz (13). For the singular elements, the equivalent consistent nodal traction is given from Eq. (A9), (A10), and (A11) as $f_i = \sigma_o/3$, $f_j = 2/3\ \sigma_o$, and $f_K = 0$. It is noted that the consistent nodal force at the crack-tip location (K's node) depends only on the slope m, i.e., we have non-zero consistent nodal tractions at the crack-tip node whenever non-uniform crack-face pressure is applied.

The solution for consistent nodal tractions with higher order pressure distributions may be easily derived using the procedures outlined above.